



Original Research Article

Synthesis of γ -Fe₂O₃ nanoparticles and catalytic activity of azide-alkyne cycloaddition reactions

K. Sudhakar^a, Avvaru Praveen Kumar^{b,c*}, Begari Prem Kumar^a, A. Raghavender^a, S. Ravi^a, Dunkana Negussa Kenie^c and Yong-Ill Lee^b

^a Rural Development Society, R&D centre, Punjagutta, Hyderabad, India, 500082

^b Department of Chemistry, College of Natural and Computational Science, Wollega University, Nekemte-P.O. Box: 395, Ethiopia

^c Department of Chemistry, Changwon National University, Changwon 641-773, Republic of Korea

ARTICLE INFORMATION

Received: 22 August 2022

Received in revised: 09 September 2022

Accepted: 14 September 2022

Available online: 01 December 2022

DOI: [10.48309/JMNC.2022.4.1](https://doi.org/10.48309/JMNC.2022.4.1)

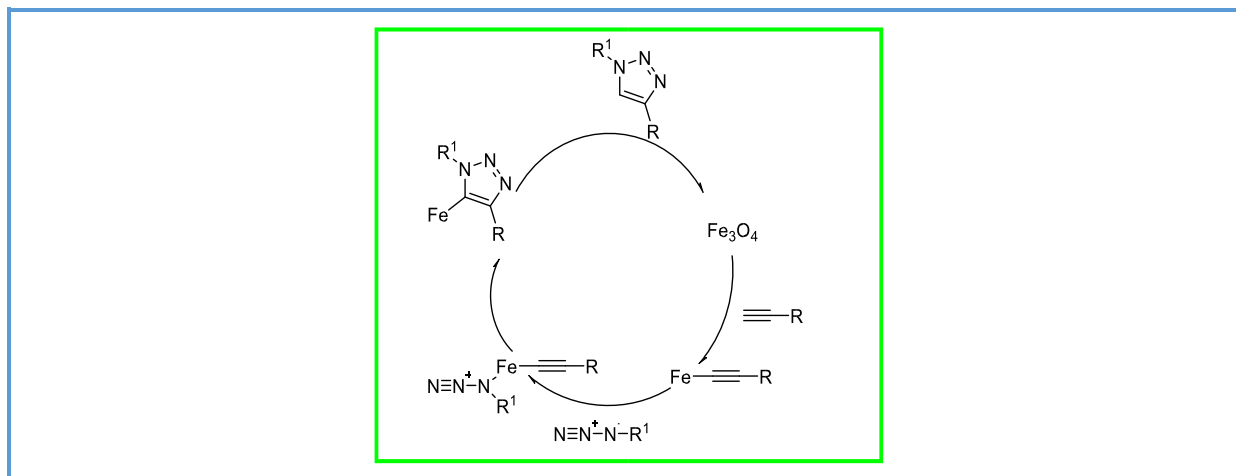
KEYWORDS

γ -Fe₂O₃ Nanoparticles
Co-precipitation method
Characterization
Catalysis

ABSTRACT

Iron nanoparticles (NPs), due to their interesting properties, low cost preparation and many potential applications in ferrofluids, magneto-optical, catalysis, drug delivery systems, magnetic resonance imaging, and biology, have attracted a lot of interest during recent years. In this research, γ -Fe₂O₃NPs were synthesized through simple co-precipitation method followed by thermal treatment at 300 °C for 2 hours. In our synthesis route, FeCl₃ and FeCl₂ were employed as precursors to synthesize γ -Fe₂O₃NPs. This approach is very effective and economical. The γ -Fe₂O₃NPs were characterized by X-ray diffraction (XRD), Fourier transform infrared (FT-IR) spectroscopy, scanning electron microscopy (SEM), transmission electron microscopy (TEM), and vibrating sample magnetometer (VSM). The XRD and FT-IR results indicated the formation of γ -Fe₂O₃NPs. The SEM and TEM images contributed to the analysis of particle size and revealed that the γ -Fe₂O₃ particle size of the nanopowders ranged from 11 and 13 nm. Magnetic property was measured by VSM at room temperature and hysteresis loops exhibited that the γ -Fe₂O₃ NPs were super-paramagnetic. The synthesized γ -Fe₂O₃NPs were applied in order to synthesize mono-triazoles within one molecule using azide-alkyne cycloaddition reactions.

Graphical Abstract



Introduction

Magnetic nanoparticles (NPs) have received significant attraction over the past decade due to their wide range of applications. Iron oxides most probably exist in three different forms in nature such as magnetite (Fe₃O₄), maghemite (γ -Fe₂O₃), and hematite (α -Fe₂O₃) [1]. The maghemite (γ -Fe₂O₃) NPs have gained considerable attention among the many known magnetic NPs because they have been used widely for the longest period of time due to their excellent properties. The γ -Fe₂O₃ NPs have been especially interesting due to their nontoxicity, thermal and chemical stability and favorable hysteric properties. The γ -Fe₂O₃ is a valuable material for mollifying biologically active compounds, bio-tagging of drug molecules, hysteretic heating of malignant cells etc. It has got a chemically active surface where a variety of bonds can be formed allowing for coating to which a variety of bio-active molecules may be attached. Its structural characteristics permit a wide range of potential applications including ferrofluids, magneto-optical and magnetic recording media, catalysis, drug delivery systems, magnetic resonance imaging, and biology [2].

A number of methods have been developed for the synthesis of γ -Fe₂O₃NPs, including the mechanochemical method [3], sol-gel process [4], laser pyrolysis [5], micro-emulsion techniques [6], thermal decomposition [7], hydro-thermal synthesis [8], flow injection synthesis [9], ball-milling [10], flame spray pyrolysis [11], sonochemistry [12], decomposition of organic precursors at high temperatures, and the oxidation of magnetite NPs [13, 14]. During the synthesis of NPs, surfactants and toxic organic solvents are often added to the solution to control the size of the γ -Fe₂O₃NPs [15]. In addition, heat treatment, such as annealing and hydrothermal processes, is often employed to improve the crystallinity and enhance the ferromagnetism [16]. However, these treatments complicate the process. Besides, from various synthesis methods, chemical co-precipitation method is studied to be the oldest, the simplest and the most desirable one to attain a large extent of homogenization together on a less particle size and quicker reaction rates [17, 18]. The chemical co-precipitation extends selection of different kinds of starting materials including simple salts to complicated organic-inorganic materials, and low cost and comfortable ones.

The primary importance of the method is the enhanced homogeneity of resulting NPs that would contribute to a kind of comparatively greater response towards catalytic activity. The catalytic activity of NPs represents a rich resource for chemical processes, employed both in industry and in academia [19]. Compounds containing a 1,2,3-triazole moiety show various biological activities such as anti-HIV-type I protease [20], antimicrobial [21], anti-allergic [22], antihyperglycemic [23] and adrenergic receptor agonists [24]. In addition, they are commercially used as photostabilizers and dyes, anticorrosive agents and agrochemicals [25]. With respect to introducing 1,2,3-triazole groups into organic molecules, the copper-catalyzed Huisgen-type alkyne-azide, cycloaddition (CuAAC), the most common “click” reaction [26, 27] has recently been used and has found wide applications in organic synthesis, materials, polymer science as well as bioconjugates, underlining its broad scope and fidelity [26, 28]. Cu(I) and Cu-based NPs have been widely used to catalyze Huisgen 1,3-dipolar cycloaddition reactions of azides [29]. Besides, copper on iron was utilized as a catalyst and scavenger for azide-alkyne cycloaddition reactions [30]. Dong *et al.* applied recyclable ruthenium(II) complex supported on magnetic NPs as regioselective catalysts for alkyne-azide cycloaddition [31].

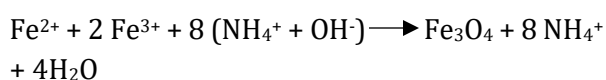
However, there has been only one report on Fe₂O₃ NPs catalyzed azide-alkyne cycloaddition reactions which includes magnetically recyclable γ -Fe₂O₃hydroxyapatite (HAP) NPs for the cycloaddition reaction of alkynes, halides and azides in aqueous media [32]. In view of wide range of transformations of alkynes catalyzed by Fe₂O₃ species, the catalytic activity of assynthesized γ -Fe₂O₃ NPs for azide-alkyne cycloadditions was assessed for the synthesis of triazoles. The present work reports a facile and efficient synthesis of γ -Fe₂O₃ NPs

using the chemical coprecipitation technique. The catalytic performances of γ -Fe₂O₃NPs were evaluated in azide-alkyne cycloaddition reactions.

Experimental

Synthesis of magnetic nanoparticles (γ Fe₂O₃ NPs)

Analytical grade chemicals and solvents were used in this research work. Metallic precursors, FeCl₃.6H₂O and FeCl₂.4H₂O (Sigma-Aldrich) were used to prepare Fe₂O₃ NPs. The typical synthesis of γ -Fe₂O₃ NPs using the chemical co-precipitation technique is described as follows. A 500 mL of deionized water was deoxygenated by bubbling N₂ gas for 30 min. A 1.0 M ammonium hydroxide was added and the mixture was stirred magnetically for 15 min under a nitrogen atmosphere. Subsequently, FeCl₃.6H₂O (1.0 M) and FeCl₂.4H₂O (1.0 M) were dropped to the solution with vigorous stirring at room temperature for 60 min. The following possible reaction was involved for the formation of Fe₃O₄ particles:



The obtained brown precipitate was collected by filtration and rinsed five times with deionized water and ethanol, respectively. Finally, the washed brown precipitate was dried at 50 °C for 10 hours in an oven. In the end, the magnetite (Fe₃O₄) nanopowder was calcined at 300 °C for 2 hours to obtain the light brown γ -Fe₂O₃ NPs.

Characterization Techniques

The XRD data of the calcined γ -Fe₂O₃ NPs were acquired using X-ray diffraction (Philips X'pert MPD 3040) with Cu K α radiation over a 2 θ range from 20° to 80° at 2.5°/min. Transmission electron microscopy (JEM 2100F)

was executed at an accelerating voltage of 200 kV on a copper grid. Scanning electron microscopy (SEM) images of the NPs were captured using a field-emission scanning electron micro analyzer (FE-SEMIRA II, LMH). Fourier transform infrared (FT-IR) spectra were recorded on a Nicolet 400 FT-IR spectrometer (Nicolet iS10, SCINCO, USA). ¹H-NMR and ¹³C-NMR spectra were recorded on a Bruker Avance-400 spectrometer. Magnetization properties of γ -Fe₂O₃ NPs were determined using a vibrating sample magnetometer (VSM) (model no. 155, serial no. 4218, USA).

Procedure for azide-alkyne cycloaddition reactions

The chemicals employed for all click reactions were purchased from commercial suppliers and used without purification. All the reactions were carried out under a N₂ atmosphere. To a solution of an azide (1.12 mmol, 1 eq) and an alkyne (1.23 mmol, 1.2 eq) in tetrahydrofuran (10 mL) was added γ -Fe₂O₃ NPs (10 mg). All the reactions were flushed with nitrogen, capped and heated to 70 °C for 6-8 hours. The reaction mixture was monitored by TLC. The catalyst was collected through filtration, washed twice with ethyl acetate (15 mL×2) and reused for next reaction. Filtrate was concentrated in vacuum using a rotary evaporator to remove organic solvents to obtain a cured compound which upon purification by column chromatography (ethyl acetate/hexane 2/6) to get corresponding products.

Product 3: N-((1-((3-(6-chloro-2Hchromen-3-yl)-1,2,4-oxadiazol-5-yl)methyl)-1H-1,2,3-triazol-4-yl)methyl)-4-methoxyaniline: White solid. mp. 169-175 °C. ¹H-NMR (CDCl₃, 400 MHz): δ 8.12 (s), 7.47 (d, J=2.5 Hz), 7.43 (s), 7.28 (dd, J=8.5 and 2.5 Hz), 6.92 (d, J=8.5 Hz), 6.89 (d, J=8.7 Hz), 6.77 (d, J=9.7 Hz), 6.13 (s, CH₂N-), 5.14 (s), 4.60 (s, CH₂NH), 3.60 (s); ¹³C-NMR (CDCl₃,

100.6 MHz): δ 174.0, 165.0, 152.7, 151.6, 145.0, 142.0, 130.6, 127.8, 126.9, 125.3, 124.5, 122.4, 119.7, 117.4, 115.4, 114.3, 63.8, 55.1, 46.3, 44.6. MS (ESI): *m/z* 450[M+H], 452 [M+H+2].
Product 4: N-((1-((3-(6-chloro-2Hchromen-3-yl)-1,2,4-oxadiazol-5-yl)methyl)-1H-1,2,3-triazol-4-yl)methyl)aniline: Light yellow solid. mp 152-155 °C. ¹H-NMR (CDCl₃, 400 MHz): δ 8.17 (s), 7.49 (d, J=2.2 Hz), 7.46 (s), 7.27 (dd, J=8.5 and 2.5 Hz), 7.07 (t, J=7.5 Hz), 6.90 (d, J=8.7 Hz), 6.63 (d, J=7.7 Hz), 6.54 (t, J=7.0 Hz), 6.16 (s, -CH₂N), 5.15 (s), 4.34 (s, -CH₂NH). ¹³C-NMR (CDCl₃, 100.6 MHz): δ 174.1, 165.0, 152.7, 148.1, 146.3, 130.6, 128.8, 127.8, 127.0, 125.3, 124.0, 122.4, 119.7, 117.4, 116.1, 112.4, 63.8, 44.6(-CH₂N-), 38.4 (-CH₂NH-); MS(ESI): *m/z* 420[M+H], 422 [M+H+2].

Product 5: 4-methyl-7-((1-phenyl-1H1,2,3-triazol-5-yl)methylamino)-2Hchromen-2-one: Pale yellow color solid, m.p: 189-191 °C. ¹H NMR (300 MHz, DMSO-*d*₆) δ (ppm): 8.09 (s, 1H), 7.60 (d, 2H, J = 7.5 Hz), 7.53 (t, 2H, J = 7.5 Hz), 7.48 (d, 1H, J = 8.6 Hz), 7.43 (t, 1H, J = 7.5 Hz), 6.70 (dd, 1H, J = 6.4, 2.3 Hz), 5.94 (s, 1H), 4.46 (d, 2H, J = 5.4 Hz), 2.36 (s, 3H);

¹³C NMR (75 MHz, DMSO-*d*₆) δ (ppm): 160.6, 155.4, 153.7, 151.8, 145.6, 138.3, 134.3, 130.2, 125.9, 121.1, 119.8, 110.4, 109.2, 107.8, 96.8, 37.9, 17.98; MS (ESI): *m/z* 333.1 [M+H]⁺.

Product 6: 7-((1-(4-methoxyphenyl)-1H-1,2,3-triazol-5-yl)methylamino)-4-methyl-2Hchromen-2-one: Light yellow solid, m.p: 168-170 °C. ¹H NMR (DMSO-*d*₆, 300 MHz) δ (ppm): 8.07 (s, 1H), 7.73-7.64 (m, 3H), 7.47 (dd, 1H, J = 6.4, 2.2 Hz), 7.43 (d, 1H, J = 2.2 Hz), 7.09 (d, 2H, J = 9.1 Hz), 6.34 (d, 1H, J = 2.2 Hz), 4.42 (d, 2H, J = 5.4 Hz), 3.96 (s, 3H), 2.51 (s, 3H); ¹³C NMR (75 MHz, DMSO-*d*₆) δ (ppm): 160.6, 159.2, 155.4, 153.5, 151.8, 145.4, 138.2, 134.4, 130.2, 125.8, 121.7, 119.8, 110.3, 109.2, 107.8, 96.7, 55.6, 37.9, 17.9; MS (ESI): *m/z* 363.1 [M+H]⁺.

Results and Discussion

The crystalline structure of the synthesized Fe_2O_3 NPs was characterized by X-ray diffraction. The X-ray diffraction (XRD) pattern of Fe_2O_3 NPs, after calcinations, was presented in Figure 1. The diffraction peaks at $2\theta = 30.58^\circ$, 35.96° , 43.61° , 54.08° , 57.58° , 63.26° , 74.64° correspond to (2 2 0), (3 1 1), (4 0 0), (4 2 2), (5 1 1), (4 4 0) and (5 3 3), respectively. The sharpness of XRD peaks reveals high crystallinity of the NPs and all the peaks matched well with standard $\gamma\text{Fe}_2\text{O}_3$ reflections. The obtained XRD pattern can be indexed as the primitive cubic system by comparison to data from $\gamma\text{Fe}_2\text{O}_3$ (JCPDS No. 39-1346) [33]. Average crystallite size is calculated to be about 1012 nm using broadening of most intense peaks from XRD pattern and Scherrer's equation.

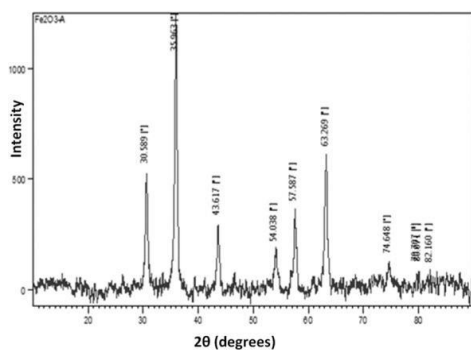


Figure 1. XRD Pattern for $\gamma\text{-Fe}_2\text{O}_3$ NPs

The surface morphology of the calcined samples of $\gamma\text{-Fe}_2\text{O}_3$ NPs was studied using TEM and SEM analysis. Figure 2a shows the SEM images of the as-prepared $\gamma\text{-Fe}_2\text{O}_3$ NPs. SEM image shows that the samples consist of particles with a nearly spherical shape and the formed $\gamma\text{-Fe}_2\text{O}_3$ NPs were agglomerated. Fig. 2b shows the TEM image of the Fe_2O_3 NPs. It can be seen that the formed NPs were of nearly spherical morphology. The $\gamma\text{-Fe}_2\text{O}_3$ NPs are moderately dispersed and the average crystallite size of particles in the range of 11 to 13 nm indicated that the homogeneous $\gamma\text{Fe}_2\text{O}_3$ NPs can be synthesized by chemical co

precipitation method at room temperature followed by thermal treatment at 300°C for 2 hours. The particle size was calculated in good agreement with the crystallite size value from XRD.

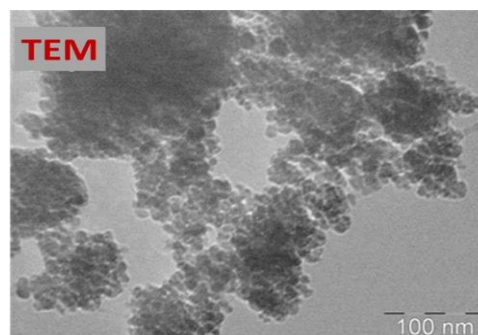


Figure 2. TEM image of $\gamma\text{-Fe}_2\text{O}_3$ NPs

The infrared spectrum (FT-IR) of the synthesized $\gamma\text{-Fe}_2\text{O}_3$ NPs was recorded in the range of $400\text{-}4000\text{ cm}^{-1}$ wave number which identify the chemical bonds as well as functional groups in the nanoparticle sample. According to Figure 3, the large broad band at 3400 cm^{-1} is ascribed to the O-H stretching vibration in -OH groups. The absorption peak around 1640 cm^{-1} could be assigned to $\delta(\text{O-H})$ vibrations in H_2O adsorbed on the material. The strong band below 642 cm^{-1} is assigned Fe-O stretching mode [34]. The band corresponding to Fe-O stretching mode of Fe_2O_3 is seen at 561 cm^{-1} [34].

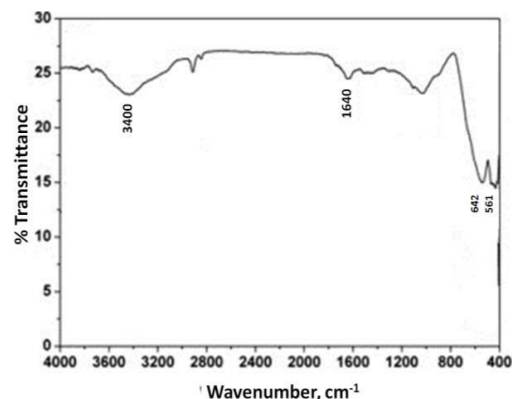


Figure 3. FT-IR Spectra of $\gamma\text{-Fe}_2\text{O}_3$ NPs

The magnetization curve for the synthesized γ -Fe₂O₃ NPs was shown in Figure 4. The curve of magnetization versus magnetic field (M–H loop) indicates that there was no hysteresis detected at the room-temperature magnetization, revealing the superparamagnetic character with zero coercivity and remanence of the synthesized γ -Fe₂O₃ NPs.

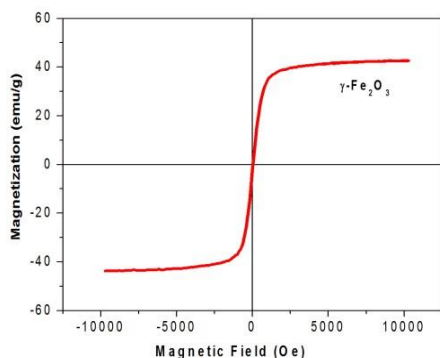


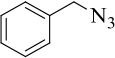
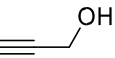
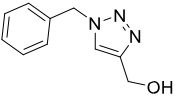
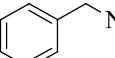
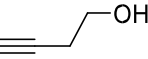
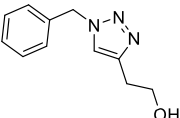
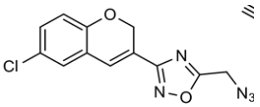
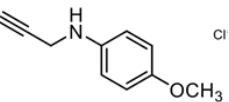
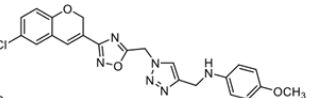
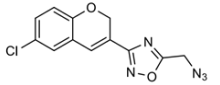
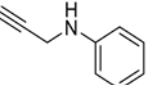
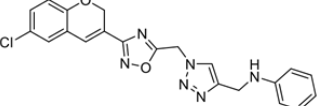
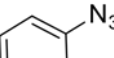
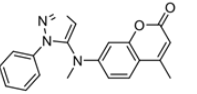
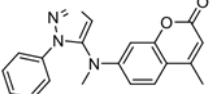
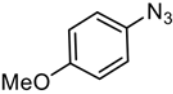
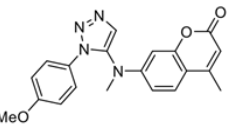
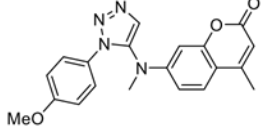
Figure 4. Magnetization curve of γ -Fe₂O₃ NPs

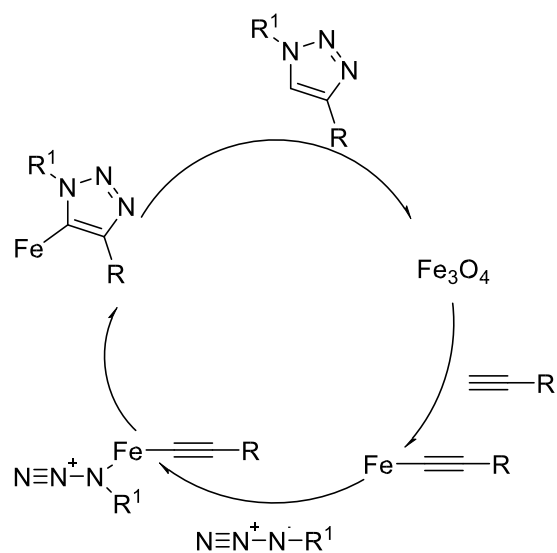
NPs catalyzed azide-alkyne cycloaddition reactions have received considerable attention during recent years [31, 32]. A magnetically separable ruthenium catalyst was synthesized through immobilizing a pentamethyl cyclopentadienyl ruthenium complex on iron oxide nanoparticles. The catalyst is highly active and selective for the synthesis of 1,5-disubstituted 1,2,3 triazoles *via* cycloaddition of alkynes and organic azides [31]. A γ -Fe₂O₃ supported on hydroxyapatite (HAP) heterogeneous catalytic system was developed to synthesize disubstituted 1,2,3-triazoles from terminal alkynes and *in situ* generated organic azide in aqueous media [32]. In the present work, we prepared mono-triazoles in one molecule using as-synthesized γ -Fe₂O₃ NPs.

Mono-triazoles were prepared by taking propyne-1-ol, butyne-1-ol and substituted alkynes on nitrogen as alkynes and benzyl azides, aryl azides and azidomethyl-2H-chrome-1,2,4-oxadiazole as azides which are shown in Table 1. The products which were obtained were characterized by ¹H-NMR and ¹³C-NMR in order to confirm the structures 1-6. Characterization report of compound 1 & 2 reported in the literature, ¹H-NMR of compound 3 peaks at δ 8.12 (s, 1H) shows the presence of triazole one olefin proton, 6.13 (s, 2H) indicates the presence of -CH₂ attached to oxadiazol function group, and the peak at 4.60 (s, 2H) indicates the presence of -CH₂-NH-. ¹H-NMR of compound 5 peaks at δ 8.09 (s, 1H) suggests the presence of triazole one olefin proton. The azide-alkyne transformations might be peculiarly relevant for drug discovery, not just because of its reliability as a linking reaction, but also because of the favorable physicochemical properties of triazoles. The proposed mechanism of the γ -Fe₂O₃ NPs catalyzed click reactions was shown in Scheme 1.

In order to make our catalytic system greener and economical, we focused on the reusability of γ -Fe₂O₃ NPs catalyst. The recyclability of the γ -Fe₂O₃ NPs catalyst was executed for 1 and 2 azide-alkyne reactions. It was received greater than 95% of the reaction products after five cycles of the reactions and does not show substantial vary in the morphology of the γ -Fe₂O₃ catalyst NPs, which indicates the repetitious catalytic performance. The catalyst was recovered quantitatively by simple filtration and reused, and gave significant activity even after the fourth cycle.

Table 1. γ -Fe₂O₃ NPs catalyzed cycloadditions of azides and alkynes

S.No	Reactants (Azide)	(Alkyne)	Product(Triazine)	Yield (%)
1				73%
2				71%
3				77%
4				73%
5				76%
6				78%

**Scheme 1.** Proposed mechanism for γ -Fe₂O₃ catalyzed click reactions

Conclusion

In this study, a simple co-precipitation method developed for synthesis of γ -Fe₂O₃NPs using FeCl₃ and FeCl₂ precursors. at 300 °C for 2 hours. The γ -Fe₂O₃NPs were characterized by XRD, FT-IR, SEM, TEM, and VSM. The SEM and TEM analyses exhibited the γ -Fe₂O₃ particle size of the nanopowders from 11 to 13 nm. Magnetic property which measured by VSM and hysteresis loops demonstrated that the γ -Fe₂O₃ NPs were super-paramagnetic. Through in hand magnetic nanoparticles of γ -Fe₂O₃NPs we synthesized mono-triazoles using azide-alkyne cycloaddition reactions in moderate yields.

Acknowledgments

KSR thanks the Rural Development society (RDS) and DST, New Delhi, India, for financial support.

Disclosure Statement

No potential conflict of interest was reported by the authors.

References

- [1]. Cornell R.M., Schwertmann U. *The Iron Oxides: Structure, Properties, Reaction, Occurrences and Uses*; WILEY-VCH Verlag GmbH Co. John Wiley & Sons, 2003 [[Google Scholar](#)], [[Publisher](#)]
- [2]. Yu S., Chow G.M. *J. Mater. Chem.*, 2004, **14**:2781 [[Crossref](#)], [[Google Scholar](#)], [[Publisher](#)]
- [3]. Tuutijärvi T., Lu J., Sillanpää M. Chen, G. *J. Hazard. Mater.*, 2009, **166**:1415 [[Crossref](#)], [[Google Scholar](#)], [[Publisher](#)]
- [4]. Cui H., Liu Y., Kusumoto R.W., Y., Abdulla-Al-Mamun, *Adv. Powder Technol.*, 2013, **24**:93 [[Crossref](#)], [[Google Scholar](#)], [[Publisher](#)]
- [5]. Miguel O.B., Morales M.P., Serna C.J., Veintemillas-Verdaguer S. *IEEE Trans. Magn.*, 2002, **38**:2616 [[Crossref](#)], [[Google Scholar](#)], [[Publisher](#)]
- [6]. Taeghwan Hyeon, Su Seong Lee, Jongnam Park, Y.C., Na, H.B. *J. Am. Chem. Soc.*, 2001, **123**:12789 [[Crossref](#)], [[Google Scholar](#)], [[Publisher](#)]
- [7]. Asuha S., Zhao S., Wu H.Y., Song L., Tegus, O. *J. Alloys Compd.*, **472**:L23 [[Crossref](#)], [[Google Scholar](#)], [[Publisher](#)]
- [8]. Islam M.S., Kurawaki J.M., Mukhlis, Bin M. *Z. J. Sci. Res.*, 2011, **4**:99
- [9]. Salazar-Alvarez G., Muhammed M., Zagorodni A.A. *Chem. Eng. Sci.*, 2006, **61**:4625 [[Crossref](#)], [[Google Scholar](#)], [[Publisher](#)]
- [10]. Randrianantoandro N., Mercier A.M., Hervieu M., Grenèche J.M. *Mater. Lett.*, 2001, **47**:150 [[Crossref](#)], [[Google Scholar](#)], [[Publisher](#)]
- [11]. Strobel R., Pratsinis S.E. *Adv. Powder Technol.*, 2009, **20**:190 [[Crossref](#)], [[Google Scholar](#)], [[Publisher](#)]
- [12]. Shafi K.V.P.M., Ulman A., Dyal A., Yan X., Yang N.L., Estournès C., Fournès L., Wattiaux A., White H., Rafailovich M. *Chem. Mater.*, 2002, **14**:1778 [[Crossref](#)], [[Google Scholar](#)], [[Publisher](#)]
- [13]. Liu T., Guo L., Tao Y., Wang Y.B., Wang W. D. *Nanostructured Mater.*, 1999, **11**:487 [[Crossref](#)], [[Google Scholar](#)], [[Publisher](#)]
- [14]. Cao S.W., Zhu Y.J., Zeng Y.P. *J. Magn. Magn. Mater.*, 2009, **321**:3057 [[Crossref](#)], [[Google Scholar](#)], [[Publisher](#)]
- [15]. Iwasaki, T., Kosaka, K., Watano, S., Yanagida, T., Kawai, T. *Mater. Res. Bull.*, 2010, **45**:481 [[Crossref](#)], [[Google Scholar](#)], [[Publisher](#)]
- [16]. Bacri, J.C., Perzynski, R., Salin, D., Cabuil, V., Massart, R. *J. Magn. Magn. Mater.*, 1986, **62**: 36 [[Crossref](#)], [[Google Scholar](#)], [[Publisher](#)]

- [17]. Kumar A.P., Kumar B.P., Kumar A.B.V.K., Huy, B.T., Lee Y.I. *Appl. Surf. Sci.*, 2013, **265**:500 [[Crossref](#)], [[Google Scholar](#)], [[Publisher](#)]
- [18]. Kumar A.P., Baek M., Sridhar C., Kumar B. P., Lee Y. *Bull. Korean Chem. Soc.*, 2014, **35**: 1144 [[Google Scholar](#)]
- [19]. Johansson J.R., Beke-Somfai, T., Stålsmeden, A.S., Kann, N. *Chem. Rev.* 2016, **23**:14726 [[Crossref](#)], [[Google Scholar](#)], [[Publisher](#)]
- [20]. da Silva F.D.C., de Souza M.C.B., Frugulhetti I.I.P., Castro H.C., Souza S.L.D.O., Moreno T., Souza L. De, Rodrigues D.Q., Souza A. M.T., Abreu P.A., Passamani F., Rodrigues C.R., Ferreira V.F. *Eur. J. Med. Chem.*, 2009, **44**:373 [[Crossref](#)], [[Google Scholar](#)], [[Publisher](#)]
- [21]. Genin M.J., Allwine D., Anderson D.J., Barbachyn M.R., Emmert D.E., Garmon S., Graber D.R., Grega K.C., Hester J.B., Hutchinson D.K., Morris J., Reischer R.J., Ford C.W., Zurenko, G.E., Hamel J.C., Schaadt R.D., Stapert D., Yagi B.H. *J. Med. Chem.*, 2000, **43**:953 [[Google Scholar](#)]
- [22]. Buckle D.R., Rockell C.J., Smith H., Spicer B.A. *J. Med. Chem.*, 1984, **27**:223 [[Crossref](#)], [[Google Scholar](#)], [[Publisher](#)]
- [23]. Alexacou K.M., Hayes J.M., Tiraidis C., Zographos S.E., Leonidas D.D., Chrysin E.D., Archontis G., Oikonomakos N.G., Paul J.V., Varghese B., Loganathan D. *Proteins*, 2008, **71**:1307 [[Crossref](#)], [[Google Scholar](#)], [[Publisher](#)]
- [24]. Brockunier L.L., Parmee E.R., Ok H.O., Candelore M.R., Cascieri M.A., Colwell L.F., Deng, L., Feeney W.P., Forrest M.J., Hom G.J., MacIntyre D.E., Tota L., Wyvratt M.J., Fisher M.H., Weber A. E. *Bioorganic Med. Chem. Lett.*, 2000, **10**:2111 [[Crossref](#)], [[Google Scholar](#)], [[Publisher](#)]
- [25]. Fan W., *Comprehensive Heterocyclic Chem. II*, vol. 4, Pergamon, Oxford: UK, 1996
- [26]. Rostovtsev V.V., Green L.G., Fokin V.V., Sharpless K.B. *Angew. Chem. Int. Ed.*, 2002, **41**:2596 [[Crossref](#)], [[Google Scholar](#)], [[Publisher](#)]
- [27]. Tornøe C. W., Christensen C., Meldal M. *J. Org. Chem.*, 2002, **67**:3057 [[Crossref](#)], [[Google Scholar](#)], [[Publisher](#)]
- [28]. Gian Cesare Tron, Tracey Pirali, Richard A. Billington, P.L.C., Giovanni Sorba A.A.G. *Med. Res. Rev.*, 2012, **29**:1292
- [29]. Steenackers H., Ermolat'ev D., Trang T.T.T., Savalia B., Sharma U.K., De Weerd A., Shah A., Vanderleyden J., Van der Eycken E.V. *Org. Biomol. Chem.*, 2014, **12**:3671 [[Crossref](#)], [[Google Scholar](#)], [[Publisher](#)]
- [30]. Kovács S., Zih-Perényi K., Révész Á., Novák Z. *Synth.*, 2012, **44**:3722 [[Crossref](#)], [[Google Scholar](#)], [[Publisher](#)]
- [31]. Wang D., Salmon L., Ruiz J., Astruc D. *Chem. Commun.*, 2013, **49**:6956 [[Crossref](#)], [[Google Scholar](#)], [[Publisher](#)]
- [32]. Kale S.R., Kahandal S.S., Gawande M.B., Jayaram R.V. *RSC Adv.*, 2013, **3**:8184 [[Crossref](#)], [[Google Scholar](#)], [[Publisher](#)]
- [33]. Grigorie A.C., Muntean C., Stefanescu M. *Thermochim. Acta*, 2015, **621**:61 [[Crossref](#)], [[Google Scholar](#)], [[Publisher](#)]
- [34]. Stoia M., Istrate R., Păcurariu C. *J. Therm. Anal. Calorim.*, 2016, **125**:1185 [[Crossref](#)], [[Google Scholar](#)], [[Publisher](#)]

How to cite this manuscript: K. Sudhakar, Avvaru Praveen Kumar*, Begari Prem Kumara, A. Raghavender, S. Ravia, Dunkana Negussa Kenie, Yong-Ill Lee. Synthesis of γ -Fe₂O₃ nanoparticles and catalytic activity of azide-alkyne cycloaddition reactions. *Journal of Medicinal and Nanomaterials Chemistry*, 4(4) 2022, 243-251. DOI: [10.48309/JMNC.2022.4.1](https://doi.org/10.48309/JMNC.2022.4.1)